Article

J. Biol. Regul. Homeost. Agents. 2024; 38(7): 5497–5506
https://doi.org/10.23812/j.biol.regul.homeost.agents.20243807.441

Microfibril-Associated Protein 2 could Regulate the Growth and Metastasis of Non-Small Cell Lung Cancer Cells via Affecting Cell Ferroptosis

Hongli Liu[1], Guanjun Ju[2,*], Yibiao Chen[2], Jie Zhang[1], Yushan Liu[3]

[1]Department of Laboratory Medicine, Tumor Hospital Affiliated to Nantong University, Nantong Tumor Hospital, 226001 Nantong, Jiangsu, China
[2]Department of Thoracic Surgery, Tumor Hospital Affiliated to Nantong University, Nantong Tumor Hospital, 226001 Nantong, Jiangsu, China
[3]Department of Pathology, Tumor Hospital Affiliated to Nantong University, Nantong Tumor Hospital, 226001 Nantong, Jiangsu, China
*Correspondence: juguanjun540@163.com (Guanjun Ju)
Submitted: 1 August 2023 Revised: 8 January 2024 Accepted: 10 January 2024 Published: 1 July 2024

Background: Microfibril-associated protein 2 (MFAP2) plays an oncogenic role in various cancer. The purpose of study is to investigate the roles of MFAP2 in non-small cell lung cancer (NSCLC).
Methods: Frist, bioinformatics were performed to determine MFAP2 expression in lung adenocarcinoma (LUAD) and Lung squamous cell carcinoma (LUSC); next, *MFAP2* mRNA expression in clinical samples has been observed using quantitative reverse transcriptase polymerase chain reaction (qRT-PCR) method, and the protein expression of MFAP2 was tested using western blot and immunohistochemistry; moreover, Receiver operating characteristic (ROC) analysis has been performed to determine the potential diagnostic value of MFAP2; furthermore, A549 as well as NCI-H1299 cells were cultured, and the cell viability, proliferation, migration as well as invasion was determined by using Cell-Counting-Kit-8 (CCK-8), colony formation assay, wound healing and Matrigel assays. Finally, the effects of MFAP2 on ferroptosis of NSCLC cells were also determined by commercially available kits or western blot methods.
Results: We found that the expression of MFAP2 was increased in NSCLC, and overexpression of MFAP2 predicted poor clinical outcomes. Furthermore, high levels of MFAP2 in tumor tissues can be used as a sensitive biomarker for NSCLC patients. Moreover, over-expression of MFAP2 may increase the growth and migration of NSCLC cells, and increased expression of MFAP2 also dampened Erastin-induced ferroptosis of A549 and NCI-H1299 ($p < 0.001$).
Conclusions: In summary, MFAP2 may worked as an oncogene in NSCLC. MFAP2 deficiency suppressed the aggressiveness of NSCLC cells by increasing the ferroptosis.

Keywords: non-small cell lung cancer; microfibril-associated protein 2; morbidity; ferroptosis

Introduction

Non-small cell lung cancer (NSCLC) characterized with high morbidity and mortality is the main subtype of lung cancer [1]. Great breakthroughs are made in anti-NSCLC therapy, however, due to the heterogeneity of the disease, the incidence of NSCLC increases annually [2] and the prognosis of NSCLC is still unsatisfactory, the 5-year survival rate is <20%, which may due to "cryptic hints" of NSCLC at early stage [3]. Therefore, to optimize the treatment plan for NSCLC is urgently needed.

Ferroptosis is a recently developed time of cell death that induced by iron-dependent phospholipid peroxidation [4]. Results of previous studies suggested that ferroptosis has been regulated by three signaling pathways: redox homeostasis (NRF2), iron handling (transferrin receptor 1 (TFR1), Ferritin heavy chain (FTH)/ferritin light chain 1 (FTL1)), mitochondrial activity and metabolism of amino acids, lipids and sugars (acyl-CoA synthetase long-chain family member 4 (ACSL4), glutathione peroxidase 4 (GPX4), solute carrier family 7 member 11 (SCL7A11), etc.) [5,6]. Iron-dependent lipid peroxidation can induce the degradation of GPX4, and consequentially promotes glutathione synthesis [7]. Moreover, cystine/glutamate antiporter SLC7A11 (Xc^-) may uptake cystine for glutathione synthesis [8]. Recently, it has been reported that Erastin-mediated inhibition of Xc^- or RAS-selective lethal 3 (RSL3)-induced blockage of GPX4 signaling can efficiently inhibit the aggressiveness behaviors of NSCLC cancer cells, resulting in increased chemosensitivity of tumor cells [9,10]. Nevertheless, the underlying mechanisms are still unclear.

Microfibril-associated protein 2 (MFAP2) is a protein component of the microfibrils [11], and it is a crucial regulator that is involved in promoting microfibril assembly and maintaining the tissue homeostasis [12]. MFAP2 possesses two forms: the extracellular part binds to extracellular matrix (ECM) proteins, while the intracellular part modulates

Journal of
BIOLOGICAL REGULATORS
and Homeostatic Agents

cell adhesion and cell morbidity [13]. Recently, increasing evidence have reported that MFAP2 is frequently found overexpressed in different type of cancers, including gastric cancer, papillary thyroid cancer and ovarian cancer etc. [14–16]. Moreover, overexpressed MFAP2 may also predict poor prognosis in patients with colorectal cancer (CRC) [17]. In lung diseases, MFAP2 is identified as a novel mesenchymal lineage marker for human lung mesenchymal progenitor cells [18]. Nevertheless, the role played by MFAP2 in NSCLC have not been elucidated. Therefore, this research designed to investigate the effects of MFAP2 on NSCLC. We hypothesized that MFAP2 can serve as a sensitive biomarker in NSCLC. To verify this, we determined cellular functions of NSCLC cells after transfecting with MFAP2 shRNA or its overexpression plasmids.

Materials and Methods

Specimens

The clinical samples have been collected from patients who went on surgical therapies at Tumor Hospital Affiliated to Nantong University from June 18, 2020 to December 31, 2022. These patients were diagnosed by two clinical doctors as NSCLC [19]. Surgical resection of cancer and adjacent tissues, low-temperature storage for subsequent experimental applications. Plasma samples collected by the Physical Examination Center of Tumor Hospital Affiliated to Nantong University as the normal control group. The inclusion and exclusion criteria for the healthy control group: Inclusion criteria for the control group: Healthy individuals were screened for physical examination items in our hospital, and no abnormalities were found in chest X-ray, abdominal ultrasound, blood routine, liver and kidney function, electrolytes, electrocardiogram, and other tests; The clinical data is complete. Exclusion criteria: (1) Suffering from malignant tumors; (2) Pregnant and lactating women; (3) Suffering from immune and blood system diseases; (4) Suffering from severe organ diseases such as heart, liver, and kidney; (5) Suffering from mental disorders and cognitive disorders; (6) Active infection. All participant received no radiotherapy or chemotherapy experience. The research has been approved by the Ethical Committee of Tumor Hospital Affiliated to Nantong University, Nantong Tumor Hospital (No. 202308226173) and in accordance with the Declaration of Helsinki. All participants provided the informed consent. Inclusion criteria: (1) patients meet the diagnostic criteria for NSCLC; (2) patients with age greater than 18 years. Exclusion criteria: (1) patients with the immunology diseases; (2) contagious diseases; (3) other tumors; (4) pulmonary diseases; (5) patients with mental disorders.

Immunohistochemistry

Tissue samples were fixed in and sliced into sections at the thickness of 4 μm, and washed after immersed in antigen repair solution. Then the sections were incubated with antibody against MFAP2 (ab183830, 1:8000, Abcam, Cambridge, MA, USA) at 4 °C overnight, followed by secondary antibody (ab150077, 1:5000, Abcam, Cambridge, MA, USA). After treated with DAB solutions and hematoxylin. The sections have been captured using a microscope. The positive rate was calculated using Image J (v 1.8.0, NIH Image, Bethesda, MD, USA).

Cell Culture

Cell line BEAS-2B, A549, HCC827, NCI-H1299, NCI-H1650, and NCI-H1688, have been obtained from ATCC (Manassas, VA, USA), which were through mycoplasma detection and str validation. BEAS-2B cells were cultured in DMEM medium containing 10% fetal bovine serum (FBS), while other cell lines were cultured in 1640 medium containing 10% FBS. All cells were cultured in a 37 °C incubator with 5% CO_2 and 95% humidity. Then A549 and NCI-H1299 cells have been cultured with 2 μM Erastin, a ferroptosis inducer, or Erastin+Ferrostatin-1, a ferroptosis inhibitor, for 48 h.

Cell Transfection

The short hairpin (sh) clones targeting MFAP2 (MFAP2 shRNAs), MFAP2 overexpression (OE) plasmids, as well as corresponding control (NC) were obtained from GeneChem (Shanghai, China). Transfecting MFAP2 shRNAs, MFAP2 OE into A549 and NCI-H1299 cells. The sequences of shRNAs were showed in **Supplementary Table 1**. The transfection efficiency was determined by polymerase chain reaction (PCR) method.

Quantitative Reverse Transcriptase Polymerase Chain Reaction (qRT-PCR)

Extract total RNA from A549 and NCI-H1299 cells, reverse record cDNA, and perform RT qPCR amplification. RT-PCR program: 95 °C, 3 seconds; 60 °C, 30 seconds; 72 °C, 15 seconds, 40 cycles, 95 °C for 30 seconds, 61 °C to 52 °C for 20 seconds, 4 cycles, each cycle dropping 3 °C; 95 °C for 30 seconds, 60 °C for 30 seconds, 35 cycles. *MFAP2* with Glyceraldehyde-3-phosphate dehydrogenase (*GAPDH*) as control. Relative *MFAP2* mRNA expression was measured with $2^{-\Delta\Delta Ct}$ method. The sequences of the primers used in PCR was as shown in **Supplementary Table 2**.

Western Blot

The total protein of A549 and NCI-H1299 cells was extracted, the protein concentration was measured, and then the protein was separated by gel electrophoresis assay and transferred to the membrane. After the membrane was sealed, it was incubated with the primary antibody matrix metalloproteinase-2 (MMP2) (ab92536, 1:5000, Abcam, Cambridge, MA, USA), MMP9 (ab76003, 1:2000, Abcam, Cambridge, MA, USA), GPX4 (ab125066, 1:2000, Abcam, Cambridge, MA, USA), FTH1 (ab183781, 1:2000, Abcam,

Cambridge, MA, USA), ACSL4 (ab155282, 1:2000, Abcam, Cambridge, MA, USA) and GAPDH (ab9485, 1:5000, Abcam, Cambridge, MA, USA) at 4 °C for 24 hours. Then incubated with HRP labeled, the second antibody at room temperature for 2 hours. The protein expression levels have been quantified by Image J. Image J converts the image into a grayscale image and analyzes the grayscale values to quantify bands.

Fe^{2+} Release

The release of ferrous iron (Fe^{2+}) was determined by an iron assay kit (cat. no. ab83366, Abcam, Cambridge, MA, USA). Briefly, following trypsinization (Trypsin (0.25%), 25200072, Thermofisher Scientific, Waltham, MA, USA), cells were resuspended. After centrifugation at 13,000 ×g, the supernatant was cultured with assay buffer. Subsequently, the release of Fe^{2+} was detected at the wavelength of 593 nm.

Determination of Superoxide Dismutase (SOD) and Glutathione (GSH)

The release of SOD and GSH was determined using the corresponding the Superoxide Dismutase Assay Kit (S0101S, Beyotime, Shanghai, China) and Glutathione Assay Kit (CS0260, Sigma-Aldrich, Shanghai, China). Briefly, after transfection or Erastin treatment, cells were lysed using lysis buffer (100 µL, Beyotime, Shanghai, China). Then the lysates were supplemented with detection buffer. Finally, the release of SOD and GSH was determined at the wavelength of 450 nm and 340 nm, respectively.

Colony Formation Assay

Cells in the logarithmic growth phase were plated on a 96-well plate (500 cells/well). Each sample had 3 wells, and the cells were continuously cultured in a cell culture incubator for about 10 days. Methanol fixation was performed, followed by staining with 0.2% crystal violet staining solution and analyze the results. The images were capture using a microscope (DM4M, Leica, Wetzlar, Germany). Colonies in predetermined fields of interest were counted (magnification, ×200).

Wound Healing Assay

Cells have been calculated in a 96-well plate (2×10^3 cells/well). Then, the cells have been scratched using a 100-µL plastic pipette tip and cultured 24 h. Then the migrated cells captured using a microscope (Leica, Germany; magnification, ×100) and quantified using Image J software and normalized to the control cells. The formulae is: wound healing rate = (initial scratch width – scratch width after 24 hours)/initial scratch width ×100%; length of cell migration (nm)/migration time (hr).

Transwell Assay

Homogeneous serum-free single-cell suspensions (1×10^5 cells/well for migration and 5×10^5/well for invasion) were added to the upper chambers, and the lower chamber was supplemented with 10% FBS. Cells in lower chamber have been fixed and stained with 1% crystal violet. Using 3% acetic acid for decolorize, completely elute crystal violet, and measure the OD value of the eluent on a Microplate reader (570 nm) to observe and quantify cell invasion. Under a 100× light microscope, select the cells passing through the membrane from: top, bottom, left, right, and center. Calculate the average value according to the formula: Migration inhibition rate = (1 – average migrating cells in the experimental group/average migrating cells in the control group) × 100%, calculate the migration ability of cells.

Detection of Reactive Oxygen Species (ROS)

Sample have been incubated with DCFDA - Cellular ROS Assay Kit (ab113851, Abcam, Cambridge, MA, USA) according to the manufacture's instructions, then washed and imaged by a fluorescence microscope. The results was quantified by selecting randomly five different fields of view using Image-Pro Plus Software 6.0 (Media Cybernetics, Bethesda, MD, USA).

Bioinformatics

MFAP2 expression in NSCLC patients was analyzed using online database Gene Expression Profiling Interactive Analysis (GEPIA)2 (http://gepia2.cancer-pku.cn/#index). Survival analysis was performed by Kaplan-Meier Plotter (http://kmplot.com/analysis/).

Statistical Analysis

All experiments were repeated 3 times. Use GraphPad Prism 9.5.1 software (Dotmatics, Boston, MA, USA) for data statistical analysis. Data all expressed as mean ± SD. Student *t* test used for analysis the differences between two groups, One-way ANOVA for multiple groups. The correlation between MFAP2 expression in tissue or plasma samples from was analyzed using Pearson's coefficient. The Receiver operating characteristic (ROC) curve was applied to analyze the potential diagnostic value of MFAP2 in NSCLC. $p < 0.05$ indicating statistically significant differences.

Results

MFAP2 is Overexpressed in NSCLC

MFAP2 functions as a positive role in tumorigenesis [11–17]. First, to verify the roles of MFAP2 in NSCLC, we screened MFAP2 expression in NSCLC patients using online database GEPIA2. We found that MFAP2 was overexpressed in both lung adenocarcinoma (LUAD) and Lung

Journal of
BIOLOGICAL REGULATORS
and Homeostatic Agents

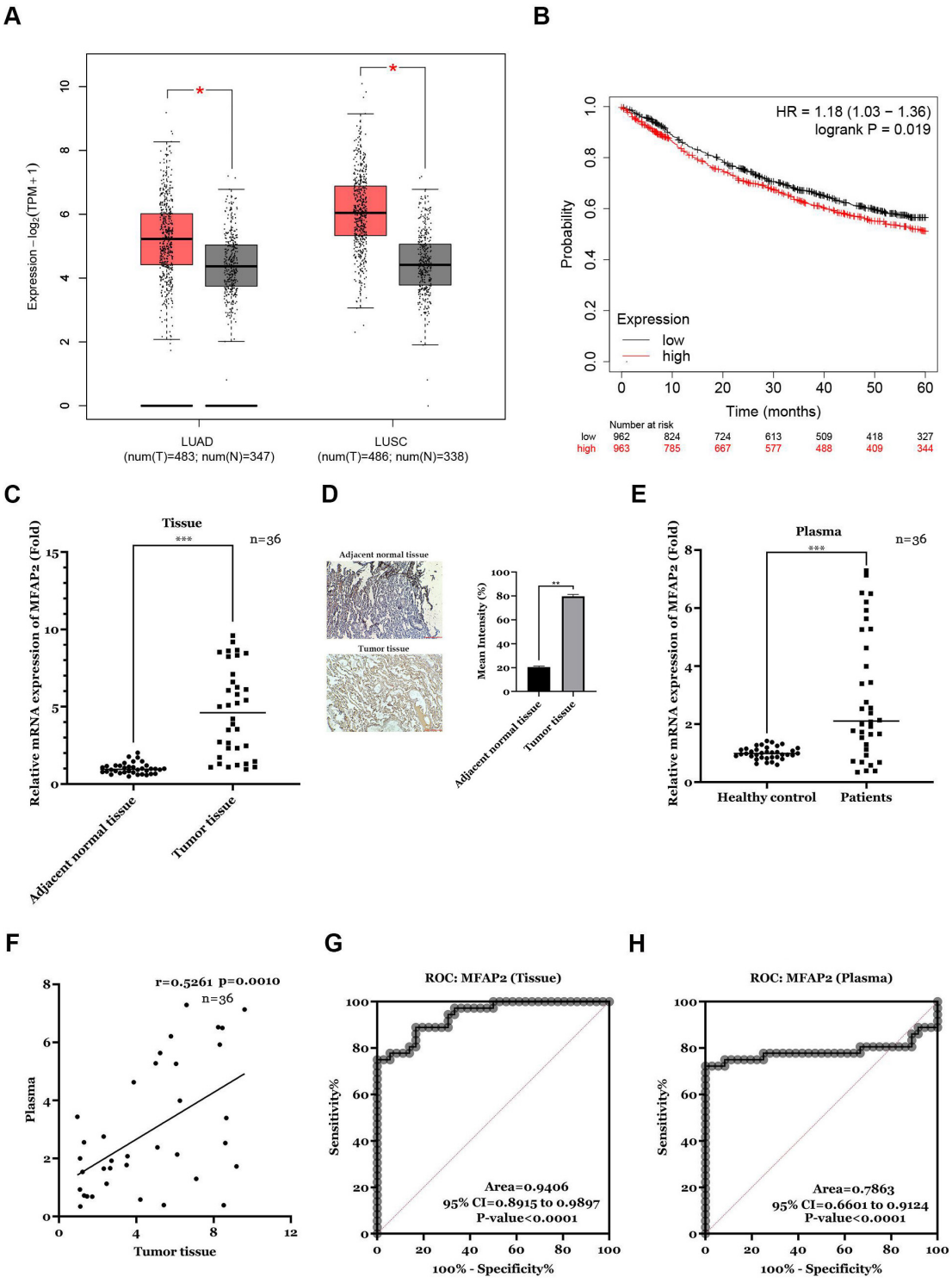

Fig. 1. MFAP2 is upregulated in NSCLC. (A) MFAP2 expression analyzed by Gene Expression Profiling Interactive Analysis (GEPIA)2. The red column on the left means the MFAP2 expression in LUAD and LUSC tumor tissue; the gray column on the right means the MFAP2 expression in LUAD and LUCS normal tissue. (B) Overall survival rates for MFAP2 low and MFAP2 high NSCLC patients by Kaplan-Meier Plotter. (C) mRNA levels of *MFAP2* in tissue samples by quantitative reverse transcriptase polymerase chain reaction (qRT-PCR). (D) MFAP2 expression in NSCLC tissue determined using immunohistochemistry (scale bar = 100 μm). (E) mRNA levels of *MFAP2* in plasma samples by qRT-PCR. (F) Correlation between MFAP2 expressions in tissue and plasma samples. (G) Receiver operating characteristic (ROC) for tissue MFAP2 in NSCLC patients. (H) ROC for plasma MFAP2 in NSCLC patients. *$p <$ 0.05, **$p < 0.01$, ***$p < 0.001$. MFAP2, Microfibril-associated protein 2; NSCLC, non-small cell lung cancer.

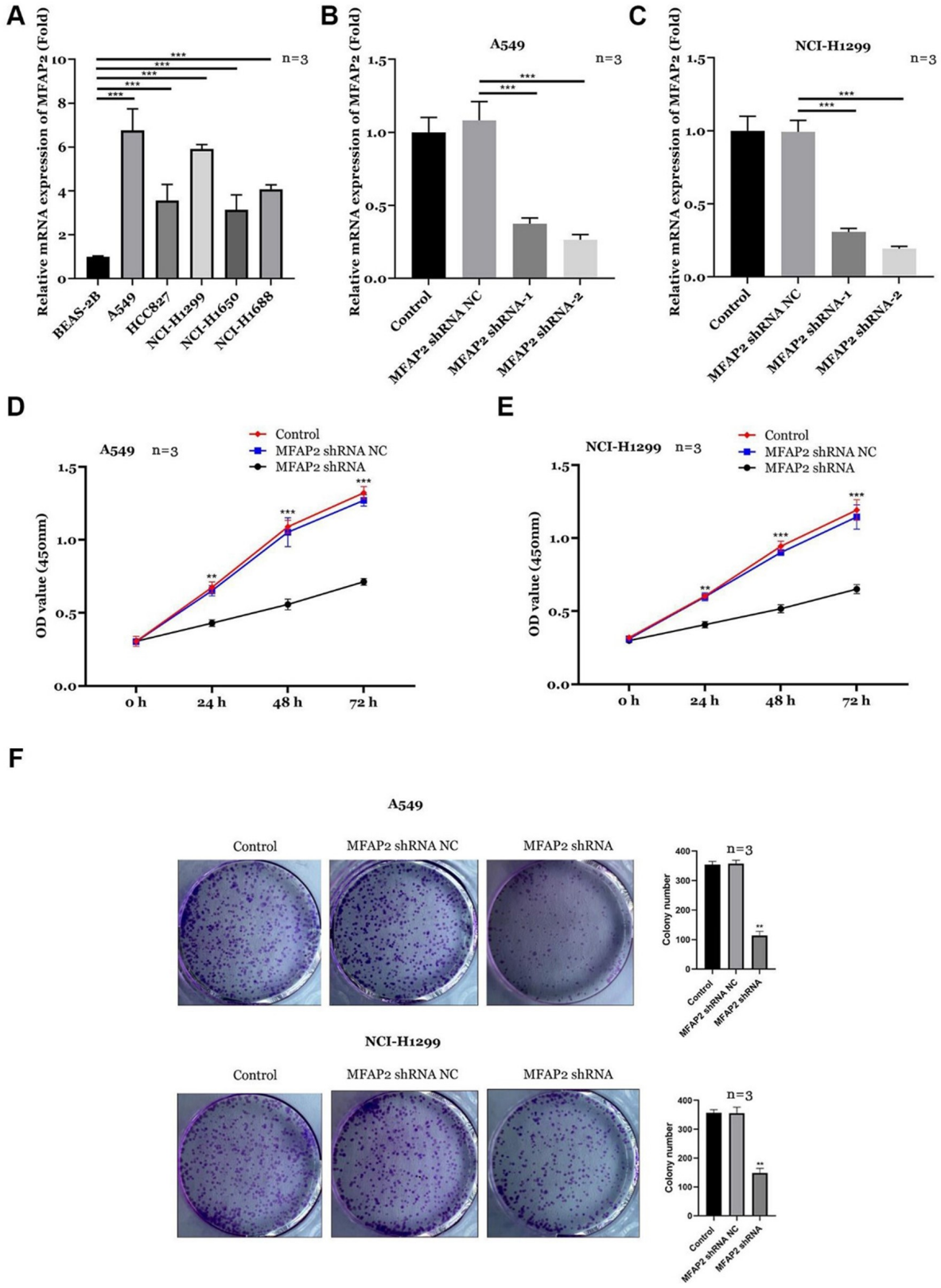

Fig. 2. MFAP2 knockdown inhibits the proliferation of A549 and NCI-H1299 cells. (A) The mRNA levels of *MFAP2*. (B,C) Transfection efficiency of MFAP2 shRNA. (D,E) Cell-Counting-Kit-8 (CCK-8). (F) Colony formation assay. n = 3. $^{**}p < 0.01$, $^{***}p < 0.001$.

Journal of
BIOLOGICAL REGULATORS
and Homeostatic Agents

squamous cell carcinoma (LUSC) ($p < 0.05$) (Fig. 1A); moreover, results of bioinformatic analysis showed that high levels of MFAP2 may predict poor 5-year overall survival rates ($p = 0.019$) (Fig. 1B). Next, to further confirm the roles of MFAP2 in NSCLC, we determined the expressions of MFAP2 in plasma or tissues that collected from NSCLC patients and healthy control. MFAP2 was markedly overexpressed in NSCLC tissues ($p < 0.001$) (Fig. 1C,D), and this was consistent with results from plasma ($p < 0.001$) (Fig. 1E). Moreover, the expression of MFAP2 in tumor tissues has been positively correlated with that from plasma from NSCLC patients (r = 0.5261, $p = 0.001$) (Fig. 1F). Additionally, results of ROC analysis showed that the AUC of MFAP2 in NSCLC tissues and plasma was 0.9406 and 0.7863, respectively (Fig. 1G,H). The above results suggested that MFAP2 can be a sensitive biomarker for NSCLC.

MFAP2 Knockdown Inhibits the Proliferation of A549 and NCI-H1299 Cells

We further determined the effects of MFAP2 shRNA on behaviors of NSCLC tumor cells. Fig. 2A showed that MFAP2 was overexpressed in all NSCLC cells, especially for A549 and NCI-H1299 cells ($p < 0.001$). Therefore, A549 and NCI-H1299 were used in the following experiments. Furthermore, Fig. 2B,C showed the transfection efficiency of MFAP2 shRNA in A549 and NCI-H1299, and MFAP2 shRNA-2, with more potent efficiency, was used in the following experiments ($p < 0.001$). Next, the effects of MFAP2 shRNA on the growth of A549 and NCI-H1299 has been determined. We found that knockdown of MFAP2 markedly decreased tumor cell viability ($p < 0.001$) (Fig. 2D,E). Additionally, MFAP2 shRNA markedly decreased tumor cell colony formation ($p < 0.01$) (Fig. 2F). These data suggested that MFAP2 may suppress the proliferation of NSCLC cells.

MFAP2 Knockdown Inhibits the Migration and Invasion of A549 and NCI-H1299

MFAP2 is a key regulator in modulating cell adhesion and morbidity [11]. Next, we determined the effects of MFAP2 shRNA migrative and invasive ability of A549 and NCI-H1299. MFAP2 knockdown markedly decreased the number of migrated A549 and NCI-H1299 at 24 h ($p < 0.01$) (Fig. 3A). Moreover, MFAP2 knockdown remarkably inhibited tumor cell invasive ability ($p < 0.01$) (Fig. 3B). Additionally, MFAP2 knockdown inhibited gelatinase (MMP2 and MMP9) expressions ($p < 0.01$) (Fig. 3C). These data suggested that MFAP2 knockdown suppressed the migration and invasion of A549 and NCI-H1299 cells.

MFAP2 Suppresses the Ferroptosis of Erastin-Treated NSCLC Cells

Finally, the effects of MFAP2 on ferroptosis of NSCLC cells have been examined. Fig. 4A showed the transfection efficiency of MFAP2 OE. MFAP2 expression was markedly increased in MFAP2 OE group in both A549 and NCI-H1299 cells, suggesting that MFAP2 OE was successfully transfected ($p < 0.001$). Next, we observed that MFAP2 overexpression markedly decreased the release of ferrous iron (Fe^{2+}) induced by Erastin treatment, while the ferroptosis inhibitor, ferrostatin-1 showed the same effects ($p < 0.001$) (Fig. 4B). On the other hand, we found that Erastin-mediated decrease of GSH and SOD was partially abrogated by MFAP2 OE ($p < 0.05$) (Fig. 4C,D), and the effects of MFAP2 OE was same as ferrostatin-1. Further, ROS production of each group was examined. We found that Erastin induced increase in ROS, and both MFAP2 OE and ferrostatin-1 decreased the ROS production ($p < 0.01$) (Fig. 4E). Moreover, Erastin also decreased the migration as well as invasion of both A549 and NCI-H1299 cells, while MFAP2 OE or ferrostatin-1 could partially alleviate the effects of Erastin ($p < 0.01$) (Fig. 4F,G). Finally, the related protein expressions were examined. We found that Erastin-mediated inhibition of protein expression of GPX4 and FTH1, as well as increased expression of ACSL4, was abrogated by overexpressed MFAP2 (Fig. 4H). Taken together, these data suggested that for Erastin treated NSCLC cells; MFAP2 over-expression may suppress the ferroptosis.

Discussion

In the present study, we found that MFAP2 was overexpressed in NSCLC and the levels of MFAP2 can be a diagnostic biomarker for NSCLC. MFAP2 knockdown suppressed the proliferative, migrative and invasive ability of A549 and NCI-H1299 cells ($p < 0.01$); however, overexpressed MFAP2 inhibited Erastin-mediated NSCLC ferroptosis ($p < 0.001$). To our knowledge, this is the first study to demonstrate the potential roles of MFAP2 in NCSLC and this may open a new light in NSCLC.

MFAP2 overexpression has been reported in many types of cancers, including gastric cancer, ovarian cancer, CRC as well as breast cancer [11,14,16,17]. In our study, we found that MFAP2 is over-expressed in NSCLC, and MFAP2 expression in tumor tissues can be a sensitive prognostic biomarker for NSCLC patients. Besides, overexpressed MFAP2 was associated with poor survival, dictating its oncogenic role in NSCLC. Moreover, MFAP2 is the key regulator that involved in cell adhesion and morbidity, suggesting that MFAP2 may endow with the capability to mediate the malignant behavior of tumor cells [11]. Results of a previous study suggested that MFAP2 promotes the morbidity of hepatocellular carcinoma [20]. Moreover, knockdown of MFAP2 inhibits the migration, inva-

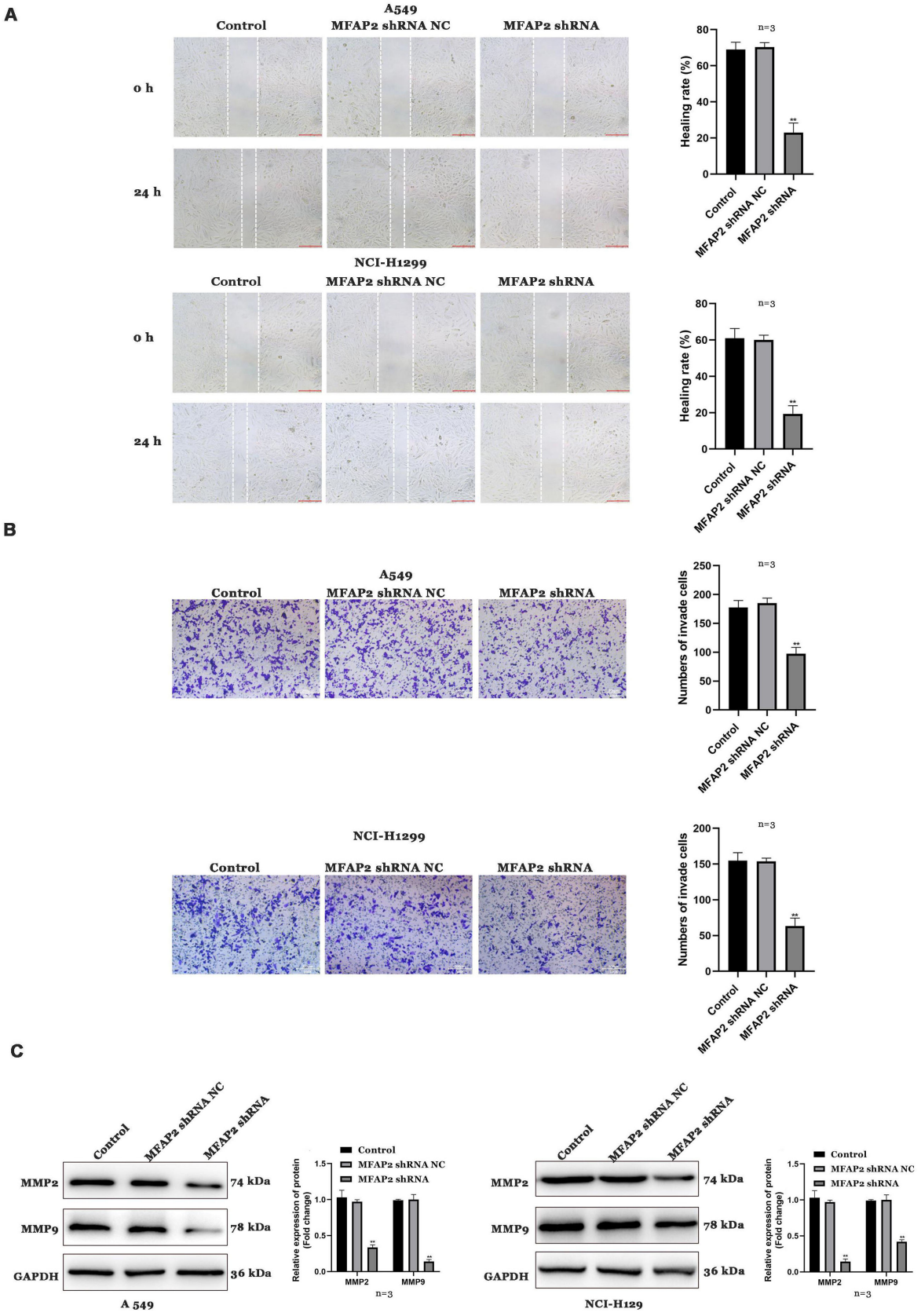

Fig. 3. MFAP2 knockdown suppresses the migration and invasion of A549 and NCI-H1299 cells. (A) Wound healing assay (scale bar = 200 μm). (B) Transwell assay (scale bar = 200 μm). (C) Western blot. n = 3. $^{**}p < 0.01$. GAPDH, Glyceraldehyde-3-phosphate dehydrogenase; MMP2, matrix metalloproteinase-2.

Journal of
BIOLOGICAL REGULATORS
and Homeostatic Agents

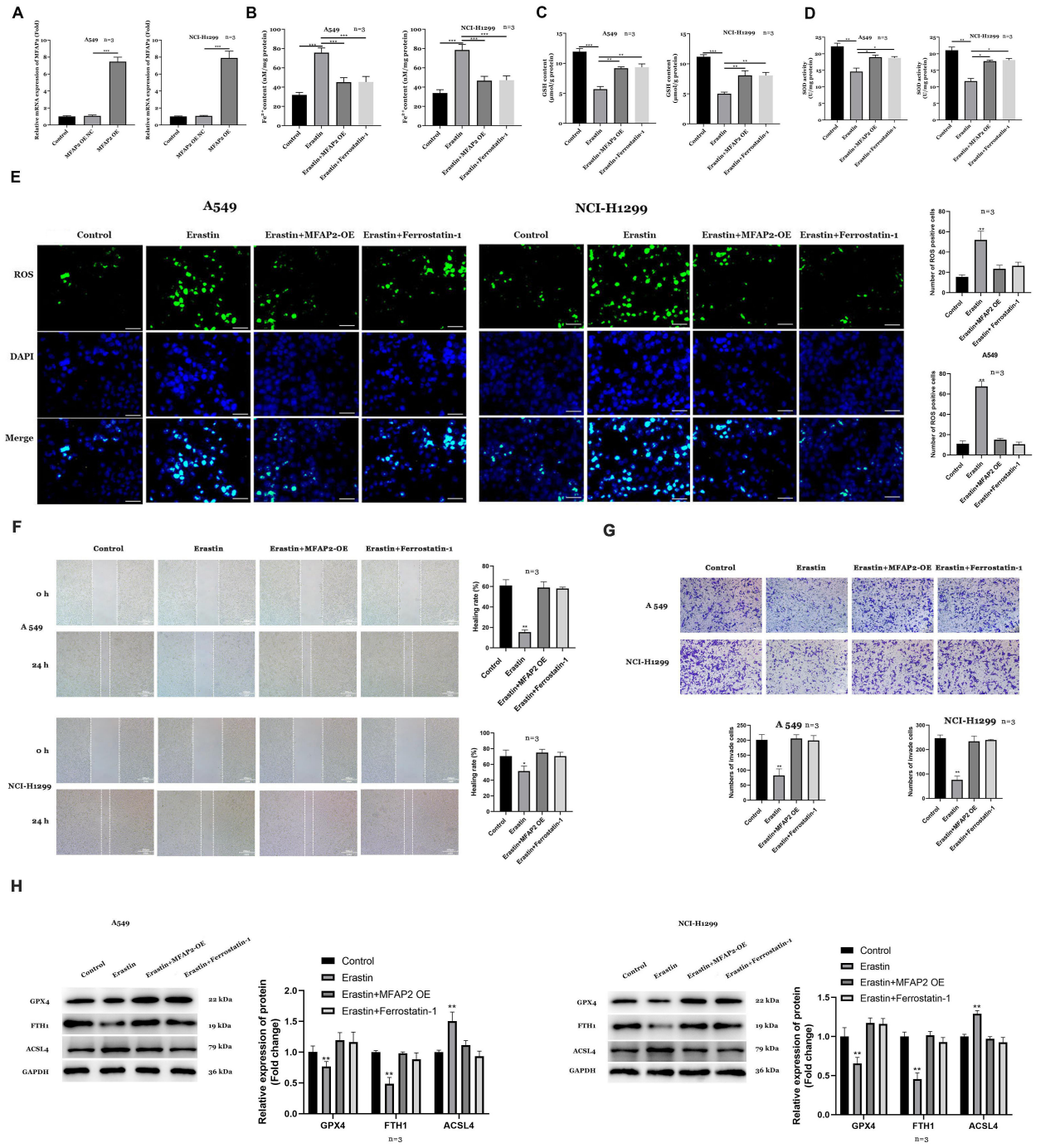

Fig. 4. MFAP2 suppresses the ferroptosis of erastin-treated NSCLC cells. (A) qRT-PCR. (B) The release of ferrous iron (Fe^{2+}). (C) Content of Glutathione (GSH). (D) Activity of Superoxide Dismutase (SOD). (E) Reactive oxygen species (ROS) production (scale bar = 200 μm). (F) Wound healing assay (scale bar = 200 μm). (G) Transwell assay (scale bar = 200 μm). (H) Western blot. n = 3. *$p < 0.05$, **$p < 0.01$, ***$p < 0.001$. FTH, Ferritin heavy chain; ACSL4, acyl-CoA synthetase long-chain family member 4; GPX4, glutathione peroxidase 4.

sion as well as metastasis of CRC and melanoma [12,17]. In this study, we found that MFAP2 knockdown inhibited the growth and metathesis of A549 and NCI-H1299 ($p < 0.01$). These findings dictated that MFAP2 can be a potential target for NSCLC, which is consistent with Xue *et al.*' study [17].

Ferroptosis is an adaptive process to eradicating the malignant cells [21]. The alteration in ferrous iron, oxidative and metabolic stress are the key factors to induce tumor cell ferroptosis. Interestingly, blocking system Xc^- (Erastin), inhibiting extracellular glutamate synthesis (RSL3), or promoting iron overload (FePt nanopar-

ticles) efficiently inhibits the malignant behaviors of tumor cells [22]. In this study, Erastin increased the accumulation of ferrous iron as well as inhibited the release of GSH and SOD. Interestingly, the blockage of system Xc^- inhibits the importing cystine; this is consistent with the results of previous reports, which is required for glutathione biosynthesis and antioxidant defense [6]. This process inhibits the release of ROS and the forming of phosphatidylethanolamines, which are vulnerable to peroxidation by iron-dependent lipoxygenases [23]. In this study, overexpressed suppressed the release of ferrous iron and promoted glutathione biosynthesis and antioxidant defense, inducing the resistance of NSCLC cells to Erastin-mediated ferroptosis ($p < 0.001$).

Recently, increasing evidences report the interconnection of ferroptosis and apoptosis, necroptosis, and pyroptosis. Apart from the crosstalk between ferroptosis and apoptosis, necroptosis, and pyroptosis, the processes of ferroptosis is distinct: (1) morphologically, ferroptosis is featured by shrunken mitochondria and reduced numbers of mitochondrial cristae, while apoptosis exhibits chromatin condensation and apoptotic body formation [22]. Pyroptosis is characterized by poor formation [24]. (2) Ferroptosis is initiated in the scenarios where ferroptosis prerequisites override antioxidant-buffering capabilities provided by ferroptosis defense systems [25,26]. This is differentiated from other form of death (caspase cascades-mediated death, RIP3/MLKL-mediated necroptosis and GSDMs-mediated pyroptosis) [27]. In this study, Erastin-mediated the release of ferroptosis prerequisites (ferrous iron) and inhibited antioxidant defense (GSH and SOD) in NSCLC cells, and the effects were dampened by MFAP2. Besides, overexpression of MFAP2 also affected the production of ROS, and the content of GPX4, FTH1 as well as ACSL4 protein. These results suggested that MFAP2 is closely related with the ferroptosis of NSCLC cells, and inhibiting MFAP2 may be a promising strategy for NSCLC. However, the underlying mechanisms still require further investigation.

Conclusions

In conclusion, MFAP2 function as an oncogene in NSCLC. MFAP2 deficiency suppressed the malignant behavior of NSCLC cells. Therefore, MFAP2 may be a novel target for NSCLC.

Availability of Data and Materials

All data included in this study are available upon request by contact with the corresponding author.

Author Contributions

HL performed most of the experiments and wrote the manuscript; YC, JZ and YL performed some of the experiments; GJ designed the study and revised the manuscript. All authors contributed to important editorial changes in the manuscript. All authors read and approved the final manuscript. All authors have participated sufficiently in the work and agreed to be accountable for all aspects of the work.

Ethics Approval and Consent to Participate

The current study has been approved by the ethic committee of Tumor Hospital Affiliated to Nantong University, Nantong Tumor Hospital (No. 202308226173) and in accordance with the Declaration of Helsinki. The informed consent was acquired from every patient.

Acknowledgment

Not applicable.

Funding

The study was supported by Nantong Municipal Health Commission Youth Medical Talent Research Fund: The role and mechanism of the interaction between SOX2 and CtBP1 in the metastasis of non-small cell lung cancer (WQ2016063); Nantong Science and Technology Plan Project: Preliminary clinical study on peripheral blood free DNA assisted diagnosis of pulmonary nodules (MSZ18215); Nantong University Clinical Medicine Special Research Fund (2023JY011).

Conflict of Interest

The authors declare no conflict of interest.

Supplementary Material

Supplementary material associated with this article can be found, in the online version, at https://doi.org/10.23812/j.biol.regul.homeost.agents.20243807.441.

References

[1] Herbst RS, Morgensztern D, Boshoff C. The biology and management of non-small cell lung cancer. Nature. 2018; 553: 446–454.
[2] Jasper K, Stiles B, McDonald F, Palma DA. Practical Management of Oligometastatic Non-Small-Cell Lung Cancer. Journal of Clinical Oncology: Official Journal of the American Society of Clinical Oncology. 2022; 40: 635–641.
[3] Duma N, Santana-Davila R, Molina JR. Non-Small Cell Lung Cancer: Epidemiology, Screening, Diagnosis, and Treatment. Mayo Clinic Proceedings. 2019; 94: 1623–1640.
[4] Tang D, Chen X, Kang R, Kroemer G. Ferroptosis: molecular mechanisms and health implications. Cell Research. 2021; 31: 107–125.
[5] Mou Y, Wang J, Wu J, He D, Zhang C, Duan C, *et al*. Ferroptosis, a new form of cell death: opportunities and challenges in cancer. Journal of Hematology & Oncology. 2019; 12: 34.
[6] Yan HF, Zou T, Tuo QZ, Xu S, Li H, Belaidi AA, *et al*. Ferrop-

Journal of
BIOLOGICAL REGULATORS
and Homeostatic Agents

tosis: mechanisms and links with diseases. Signal Transduction and Targeted Therapy. 2021; 6: 49.

[7] Liang D, Minikes AM, Jiang X. Ferroptosis at the intersection of lipid metabolism and cellular signaling. Molecular Cell. 2022; 82: 2215–2227.

[8] Lin W, Wang C, Liu G, Bi C, Wang X, Zhou Q, *et al*. SLC7A11/xCT in cancer: biological functions and therapeutic implications. American Journal of Cancer Research. 2020; 10: 3106–3126.

[9] Chen X, Kang R, Kroemer G, Tang D. Broadening horizons: the role of ferroptosis in cancer. Nature Reviews. Clinical Oncology. 2021; 18: 280–296.

[10] Müller F, Lim JKM, Bebber CM, Seidel E, Tishina S, Dahlhaus A, *et al*. Elevated FSP1 protects KRAS-mutated cells from ferroptosis during tumor initiation. Cell Death and Differentiation. 2023; 30: 442–456.

[11] Gong X, Dong T, Niu M, Liang X, Sun S, Zhang Y, *et al*. lncRNA LCPAT1 Upregulation Promotes Breast Cancer Progression via Enhancing MFAP2 Transcription. Molecular Therapy. Nucleic Acids. 2020; 21: 804–813.

[12] Chen Z, Lv Y, Cao D, Li X, Li Y. Microfibril-Associated Protein 2 (MFAP2) Potentiates Invasion and Migration of Melanoma by EMT and Wnt/β-Catenin Pathway. Medical Science Monitor: International Medical Journal of Experimental and Clinical Research. 2020; 26: e923808.

[13] Qiu Z, Xin M, Wang C, Zhu Y, Kong Q, Liu Z. Pan-Cancer Analysis of Microfibrillar-Associated Protein 2 (MFAP2) Based on Bioinformatics and qPCR Verification. Journal of Oncology. 2022; 2022: 8423173.

[14] Shan Z, Wang W, Tong Y, Zhang J. Genome-Scale Analysis Identified NID2, SPARC, and MFAP2 as Prognosis Markers of Overall Survival in Gastric Cancer. Medical Science Monitor: International Medical Journal of Experimental and Clinical Research. 2021; 27: e929558.

[15] Dong SY, Chen H, Lin LZ, Jin L, Chen DX, Wang OC, *et al*. MFAP2 is a Potential Diagnostic and Prognostic Biomarker That Correlates with the Progression of Papillary Thyroid Cancer. Cancer Management and Research. 2020; 12: 12557–12567.

[16] Zhao LQ, Sun W, Zhang P, Gao W, Fang CY, Zheng AW. MFAP2 aggravates tumor progression through activating FOXM1/β-catenin-mediated glycolysis in ovarian cancer. The Kaohsiung Journal of Medical Sciences. 2022; 38: 772–780.

[17] Xue M, Mi S, Zhang Z, Wang H, Chen W, Wei W, *et al*. MFAP2, upregulated by m1A methylation, promotes colorectal cancer invasiveness via CLK3. Cancer Medicine. 2023; 12: 8403–8414.

[18] Danopoulos S, Bhattacharya S, Mariani TJ, Al Alam D. Transcriptional characterisation of human lung cells identifies novel mesenchymal lineage markers. The European Respiratory Journal. 2020; 55: 1900746.

[19] Oncology CSoC. Guidelines of Chinese Society of Clinical Oncology (CSCO)-Non-Small Cell Lung Cancer. 2023. Available at: http://www.csco.ac.cn/. Accessed: 28 September 2023.

[20] Zhang N, Shao F, Jia W. Upregulation of microfibrillar-associated protein 2 is closely associated with tumor angiogenesis and poor prognosis in hepatocellular carcinoma. Oncology Letters. 2021; 22: 739.

[21] Yang WS, Stockwell BR. Ferroptosis: Death by Lipid Peroxidation. Trends in Cell Biology. 2016; 26: 165–176.

[22] Friedmann Angeli JP, Schneider M, Proneth B, Tyurina YY, Tyurin VA, Hammond VJ, *et al*. Inactivation of the ferroptosis regulator Gpx4 triggers acute renal failure in mice. Nature Cell Biology. 2014; 16: 1180–1191.

[23] Dixon SJ, Lemberg KM, Lamprecht MR, Skouta R, Zaitsev EM, Gleason CE, *et al*. Ferroptosis: an iron-dependent form of non-apoptotic cell death. Cell. 2012; 149: 1060–1072.

[24] Yu P, Zhang X, Liu N, Tang L, Peng C, Chen X. Pyroptosis: mechanisms and diseases. Signal Transduction and Targeted Therapy. 2021; 6: 128.

[25] Soula M, Weber RA, Zilka O, Alwaseem H, La K, Yen F, *et al*. Metabolic determinants of cancer cell sensitivity to canonical ferroptosis inducers. Nature Chemical Biology. 2020; 16: 1351–1360.

[26] Ingold I, Berndt C, Schmitt S, Doll S, Poschmann G, Buday K, *et al*. Selenium Utilization by GPX4 Is Required to Prevent Hydroperoxide-Induced Ferroptosis. Cell. 2018; 172: 409–422.e21.

[27] Galluzzi L, Vitale I, Aaronson SA, Abrams JM, Adam D, Agostinis P, *et al*. Molecular mechanisms of cell death: recommendations of the Nomenclature Committee on Cell Death 2018. Cell Death and Differentiation. 2018; 25: 486–541.